JOURNAL OF GEOPHYSICAL RESEARCH, VOL. 90, NO. B10, PAGES 8707–8717, SEPTEMBER 10, 1985

Secular Variation, Crustal Contributions, and Tectonic Activity in California, 1976–1984

M. J. S. JOHNSTON, S. A. SILVERMAN, R. J. MUELLER, AND K. S. BRECKENRIDGE

U.S. Geological Survey, Menlo Park, California

Five to ten years of data from an array of 34 total field magnetometers are used to define the temporal and spatial characteristics of secular variation throughout central and southern California. For this period, well-determined rates of secular variation are obtained at each site. These rates are temporally linear but spatially variable, ranging from −45 nT/a near San Francisco to −54 nT/a near the Mexican border. Least squares analysis of all data indicates secular variation decreases in a general southeasterly direction according to $\dot{F} = k_1*\theta + k_2*\phi + K$, where $\dot{F}$ is in nanoteslas per year, θ and ϕ are the geographic latitude and longitude, and k_1, k_2, and K are 1.66 ± 0.13 nT/a deg, −0.13 ± 0.10 nT/a deg, and −123.2 ± 0.2 nT/a, respectively. Deviations of as much as 1 nT/a occur on scales of a few tens of kilometers. These apparent small-scale secular variation anomalies result, in part, from differences in local induction and remanent magnetization and may be reduced by determination of a site transfer function. A planar surface fit to the corrected data has the form $\dot{F} = k_1*\theta + k_2*\phi + K$, where k_1, k_2, and K are now 1.50 ± 0.08 nT/a deg, −0.23 ± 0.06 nT/a deg, and −129.2 ± 0.1 nT/a, respectively. Residual field variations obtained after correction of all data for secular variation are most apparent on the San Andreas fault in southern California between Palm Springs and the Salton Sea and marginally so along the recent Coyote (M_L = 5.9 of August 6, 1979) and Morgan Hill (M_L = 5.8 of April 24, 1984) aftershock zones. These residuals could be explained by stress localization in these regions and, particularly in the case of the southern San Andreas anomaly, may indicate the location of a future damaging earthquake. Incomplete correction for complex site effects may be an alternative explanation. In the first large-scale test of global secular variation models we find that the models for this region do not predict either the amplitudes or the mean isogram directions of these data to better than several tens of nanoteslas per year and several tens of degrees, respectively. This may result from a failure to correct for site response effects at some observatories before using the data in global spherical harmonic expansions. Local magnetization response can therefore bias estimates of secular variation and yield apparent impulsive behavior when external fields are perturbed.

1. INTRODUCTION

Secular variation of the earth's geomagnetic field, first recognized by Gellibrand in 1635 [*Chapman and Bartels*, 1940], is generally considered to result from magnetohydrodynamic processes in the earth's core [*Elsasser*, 1950; *Bullard et al.*, 1950]. Determination of secular variation at the earth's surface is complicated by poorly understood crust and upper mantle sources usually termed small-scale secular variation [*Shapiro and Johnston*, 1979]. Some minor contributions to drift terms in the geomagnetic field are generated in the ionosphere and magnetosphere and from solar cycle effects. Because secular variation provides information about the geomagnetic dynamo and core-mantle coupling processes and because secular variation must be predicted and removed from survey data, its characteristics have been studied extensively. At this point, however, neither the geomagnetic models based on data from the present number and distribution of magnetic observatories [*Yukutake and Tachinaka*, 1969; *Peddie*, 1981, 1982; *Peddie and Fabiano*, 1982] nor those derived from satellite data [*Regan et al.*, 1975; *Langel et al.*, 1981; *Cain et al.*, 1983, 1984] are detailed enough to separate and display the small-scale character and temporal variation of secular variation.

In this paper we report the first measurements of secular variation obtained from a dense array of magnetometers in California and compare these data with predictions from global secular variation models. These measurements show that contributions from induction sources and magnetization effects in the crust can contaminate secular variation estimates. We suggest a method for identifying and reducing these effects in data used for secular variation modeling. These techniques are applied to the Californian array data, and the residuals are discussed in terms of possible tectonomagnetic sources along the San Andreas fault.

The array of synchronized proton magnetometers has been operating along the San Andreas fault in California since 1973 [*Johnston et al.*, 1976]. The maximum extent of this array is now 788 km in a northwest-southeast direction. Precise magnetic field measurements have also been made at least once per year at several hundred other benchmarks. The measurement precision is less than 0.2 nT for hour averages over 10-km baselines [*Johnston et al.*, 1984]. The original intent of this experiment was to identify local magnetic fields generated by perturbations in the state of crustal stress [*Stacey and Johnston*, 1972]. The amplitude of the expected tectonomagnetic effects is a few nanoteslas [*Johnston*, 1978].

For the tectonomagnetic experiment, secular variation and other geomagnetic field transients must be identified and removed from the measurements. Because of the scale of the array, the time history of the data, and, in particular, the effort that has gone into understanding the details of point magnetic field measurements [*Davis and Johnston*, 1983], the array can alternatively be used to investigate secular variation in this region. The purpose of this paper is to (1) define spatial character and temporal changes of secular variation in California for the period 1976 to 1984, (2) identify the degree to which crustal magnetization distorts secular variation estimates in this region, (3) search the corrected data for anomalies of tectonic origin, and (4) compare these corrected data to predictions from global secular variation models to estimate the model precision.

Paper number 4B5265.

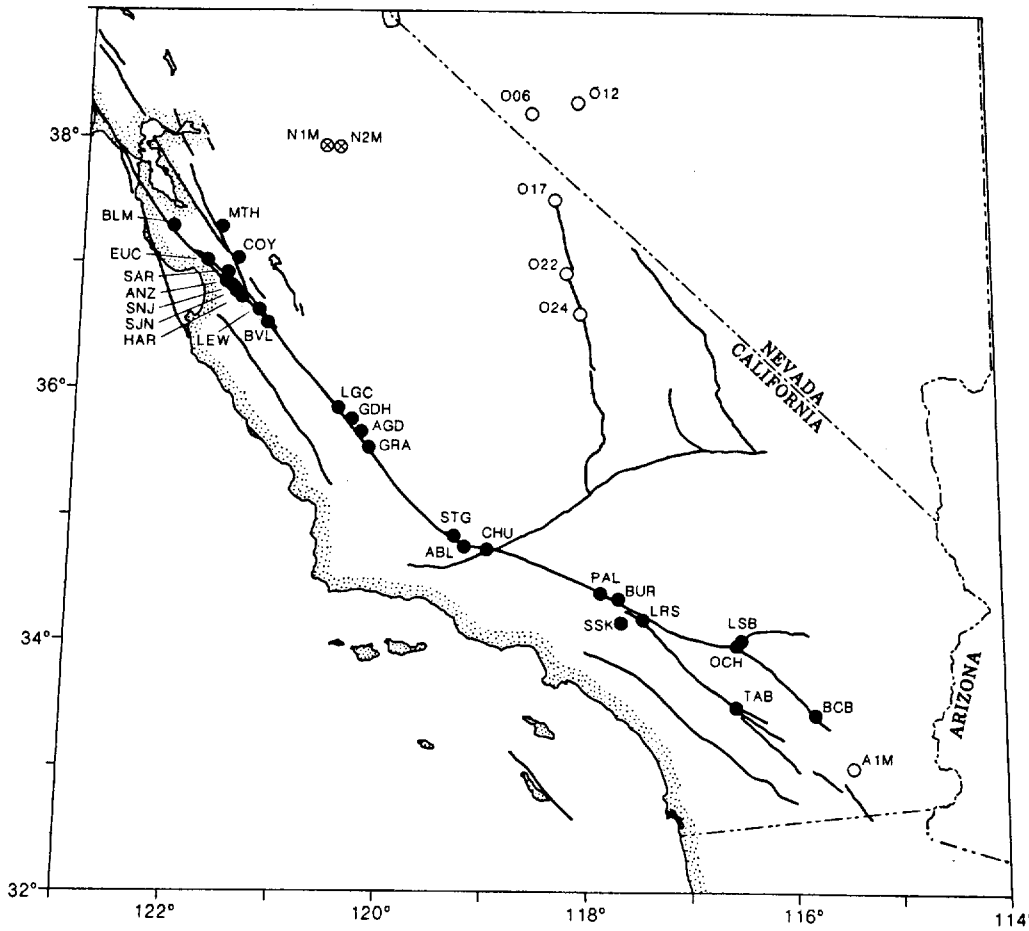

Fig. 1. Sites in California and Nevada where synchronized magnetic field measurements are made continuously or periodically. Magnetometers with digital telemetry are shown as solid circles, 5-day portables are shown as circled crosses, and survey measurements are shown as open circles.

2. Sites and Instrumentation

Figure 1 shows the locations of sites in California and Nevada where synchronized total field measurements have been recorded since 1973. All measurements are taken at a sensitivity of 0.25 nT. Twenty-six permanent sites (solid circles) telemeter digital data on the hour and every 10 min thereafter to a computer at the U.S. Geological Survey (USGS) in Menlo Park, California. Three-component data are also recorded at site HAR. Additional synchronized measurements are obtained annually or biannually with portable digital recorders, either installed at fixed sites (circled crosses) for five days or sampling continuously at fixed sites (open circles) during a 10-min period. All sensors are placed in permanent sensor holders, with repositioning better than 1 cm. All sites were carefully selected to have horizontal and vertical gradients across the measurement point less then 3 nT/m. *Mueller et al.* [1981] provide a complete description of measurement techniques and installation and checking procedures. For typical site separations of 10-km, differential field measurement precisions at a 10-min sample interval are 0.25, 0.2, and 1.5 nT for telemetered, 5-day survey, and 10-min survey data, respectively [*Johnston et al.*, 1984].

3. Data

A summary of 5-day means of total field data from telemetered instruments is shown in Figure 2. The obvious features in the data are magnetic storm effects and long-term linear trends or secular variation. Because of the clear linear character of secular variation during this period, least squares linear fits were determined for each data set from 1976 to 1984 when the best coverage and the most complete and linear data were obtained. Table 1 summarizes these secular variation rates and their estimated errors as a function of site latitude and longitude. To obtain better two-dimensional coverage, secular variation rates obtained from some of the repeated survey sites are also included in Table 1. These sites were chosen from areas of low crustal magnetization because sites with high local magnetization also have perturbed inclination and declination values and the data obtained usually require correction. This is demonstrated in Figure 3, in which the lower three traces show total field, inclination, and declination at the various sites as a function of distance from San Francisco.

It is clear from Table 1 that the rates vary from about -44.7 nT/a in the northwest to about -53.9 nT/a in the southeast. These data can be fit with a minimum total curvature contouring program that is equivalent to a cubic spline interpolation [*Briggs*, 1974]. The results are shown in Figure 4*a*. A grid interval of 30 km was used to minimize high-order fitting in regions of high station density. The contour structure is still complex in regions where the data density is high in spite of the inherent averaging imposed by the 30-km grid interval, indicating spatial nonuniformities in secular variation on scales from several hundreds of kilometers down to the

grid interval. Closer inspection indicates that these spatial nonuniformities in these raw data occur on scales down to the smallest site separation, 3.5 km. These effects are generally termed small-scale secular variation [*Shapiro and Johnston*, 1979].

4. Crustal Contributions

It is evident from Table 1 that sites only 10 km apart can have either similar secular variation rates, as expected from sources in the core (e.g., sites BVL and LEW), or rates differing by as much as 1.0 nT/a (e.g., sites AGD and GRA). We suggest that at least some of these local variations result not from complexity in secular variation but from differences in local magnetic induction response at the various sites. To clarify this issue, we need to discuss the relative importance of the various contributions to apparent secular variation at a particular site.

In addition to magnetic induction differences, apparent contributions to secular variation could result from electrical induction in different conductivity structures and from the stress sensitivity of crustal rocks [*Stacey and Johnston*, 1972]. Electrical induction is a frequency dependent effect which has a penetration or skin depth given by

$$D = (2/\omega\mu\sigma)^{1/2} \quad (1)$$

where σ is the conductivity, ω is the angular frequency, and μ is the permeability of the crust.

Electrical induction is not expected to provide any significant contributions to secular variation measurements for two reasons. First, induction currents at very long periods will have large (global) scales and are unlikely to cause sustained fields on scales of a few kilometers. Furthermore, it is difficult to maintain these currents at appreciable levels for many years. Second, in central California where we observe the greatest difference in secular variation rates, a recent investigation of comparative site response indicates that there were no significant phase lags for periods of one day and longer [*Davis and Johnston*, 1983]. Phase lags would be expected if frequency dependent induction effects were occurring.

At periods less than one day, induction effects do occur. These are primarily at ocean tidal M_2 and S_2 periods and have amplitudes of about 1 nT [*Johnston et al.*, 1983]. Longer-term ocean currents have amplitudes much less than those at the dominant tidal periods. The induction fields would be correspondingly smaller.

It is also unlikely that many of the differences in secular variation are due to accumulating crustal stress, even though the regions in central and southern California are tectonically and seismically active. Crustal strain measured in these areas indicates a fairly uniform accumulation of about 0.3 μstrain/a [*Prescott et al.*, 1979]. Even with the most optimistic tectonomagnetic models we would not expect to obtain contributions of more than 0.5 nT/a from these causes [*Johnston*, 1978]. Of course, concentrated strain accumulation and release in localized zones from earthquake or fault activity may produce anomalies of approximately 1 nT if tectonomagnetic effects take place. These would be of limited extent unless major failure occurs or is about to occur. If tectonomagnetic events occur linearly with time, they could not easily be distinguished from small-scale secular variation.

The primary contribution from crustal sources comes therefore from the remanent and induced magnetization of the crustal rocks. As pointed out by *Davis and Johnston* [1983], variable crustal susceptibility causes contrasting magnetic induction at different sites (the "susceptibility effect"). Combined variable remanence and susceptibility leads to field vectors with different orientations at different sites (the "orientation effect"). In simple terms, the static field (i.e., the vector sum of the dipole field, remanent fields, and induced fields) at a site is different in amplitude and direction from that at an adjacent site because the remanent and induced field vectors are different. The application of a uniform disturbance field (and its induced component) will therefore produce a different net effect at each site. Changes in disturbance fields (such as from solar flare activity, etc.) will create apparent changes in secular variation, diurnal variation, etc. because of these site response effects.

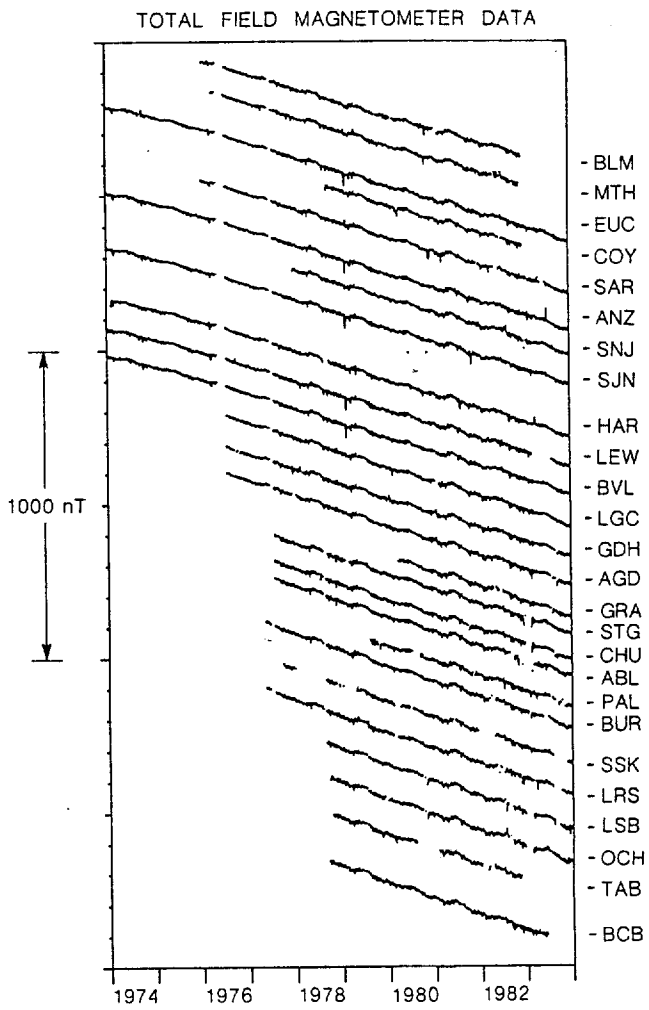

Fig. 2. Total magnetic field time histories from northwest to southeast along the San Andreas Fault.

Site response effects have been calculated for all of the California stations with continuous telemetered data in the manner used by *Davis and Johnston* [1983]. The Fischer F test was used to test the relative significance of the Wiener coefficients. In contrast to the results obtained by *Davis et al.* [1981], significant coefficients derived from known forcing functions (magnetic storms) were found for hourly averages of the field data at zero lag only. Coefficients for a lag of one or more were significant only at the 80% to 90% level or less. At zero lag, $\delta F_i \approx A\ \delta X_i + B\delta Y_i + C\ \delta Z_i$, where δF_i is the detrended total field data referenced to HAR total field data during storm periods, δX_i, δY_i, and δZ_i are the corresponding

TABLE 1. Observed and Corrected Secular Variation From Sites in the Magnetometer Array

Site	Latitude	Longitude	Secular Variation, nT/a		Correction, nT/a	Residual, nT/a
			Observed	Corrected		
BLM	37.319	−122.151	−44.778 ± 0.008	−44.990 ± 0.008	−0.212	−0.375
MTH	37.322	−121.667	−45.677 ± 0.009	−45.400 ± 0.009	+0.277	−0.676
COY	37.072	−121.503	−45.091 ± 0.017	−45.727 ± 0.017	−0.636	−0.590
EUC	37.053	−121.805	−45.860 ± 0.005	−45.188 ± 0.005	+0.672	−0.093
SAR	36.956	−121.592	−46.162 ± 0.006	−45.456 ± 0.006	+0.706	−0.165
ANZ	36.886	−121.596	−46.476 ± 0.005	−45.002 ± 0.005	+1.474	0.393
SNJ	36.850	−121.550	−46.000 ± 0.009	−45.951 ± 0.009	+0.049	−0.492
SJN	36.819	−121.509	−45.175 ± 0.006	−45.059 ± 0.004	+0.116	0.457
HAR	36.775	−121.454	−46.673 ± 0.005	−45.937 ± 0.005	+0.736	−0.343
LEW	36.673	−121.279	−46.834 ± 0.005	−45.745 ± 0.005	+1.089	0.044
BVL	36.572	−121.193	−46.900 ± 0.004	−46.144 ± 0.004	+0.756	−0.184
LGC	35.910	−120.482	−47.855 ± 0.006	−47.609 ± 0.006	+0.246	−0.489
GDH	35.829	−120.341	−47.770 ± 0.007	−47.451 ± 0.007	+0.319	−0.176
AGD	35.730	−120.244	−48.652 ± 0.007	−47.526 ± 0.007	+1.126	−0.080
GRA	35.603	−120.173	−49.606 ± 0.017	−47.185 ± 0.017	+2.421	0.468
STG	34.917	−119.336	−49.320 ± 0.009	−48.806 ± 0.009	+0.514	0.073
ABL	34.833	−119.229	−48.967 ± 0.009	−49.191 ± 0.009	−0.224	−0.161
CHU	34.810	−119.012	−49.275 ± 0.008	−49.263 ± 0.008	+0.012	−0.148
PAL	34.459	−117.898	−49.186 ± 0.016	−49.718 ± 0.016	−0.532	0.185
BUR	34.410	−117.732	−51.316 ± 0.008	−49.987 ± 0.008	+1.329	0.028
LRS	34.244	−117.494	−50.948 ± 0.008	−50.752 ± 0.008	+0.196	−0.432
SSK	34.220	−117.696	−50.198 ± 0.014	−50.374 ± 0.014	−0.176	−0.065
LSB	34.065	−116.548	−51.329 ± 0.012	−50.003 ± 0.012	+1.326	0.807
OCH	34.029	−116.600	−51.769 ± 0.012	−49.919 ± 0.012	+1.850	0.933
TAB	33.543	−116.605	−50.700 ± 0.017	−51.157 ± 0.017	−0.457	0.423
BCB	33.475	−115.855	−51.898 ± 0.014	−51.300 ± 0.014	+0.598	0.558
012	38.371	−118.133	−45.240 ± 0.02	−45.240 ± 0.02	0	−1.264
006	38.283	−118.600	−44.080 ± 0.02	−44.080 ± 0.02	0	−0.081
N1M	37.996	−120.656	−42.560 ± 0.02	−42.560 ± 0.02	0	1.389
N2M	37.991	−120.513	−41.565 ± 0.02	−41.565 ± 0.02	0	2.424
017	37.590	−118.374	−45.430 ± 0.02	−45.430 ± 0.02	0	−0.338
022	37.000	−118.250	−45.750 ± 0.02	−45.750 ± 0.02	0	0.257
024	36.681	−118.114	−47.360 ± 0.02	−47.360 ± 0.02	0	−0.843
A1M	33.050	−115.504	−53.889 ± 0.02	−53.889 ± 0.02	0	−1.311

The observed values were obtained by least squares linear fits to the data during the period 1976 to 1984 from sites shown in Figure 1. Corrected secular variation values were determined using the coefficients in Table 2. Also included are the correction values at each site and the residuals at each site after subtracting a planar fit from the corrected data as described in the text.

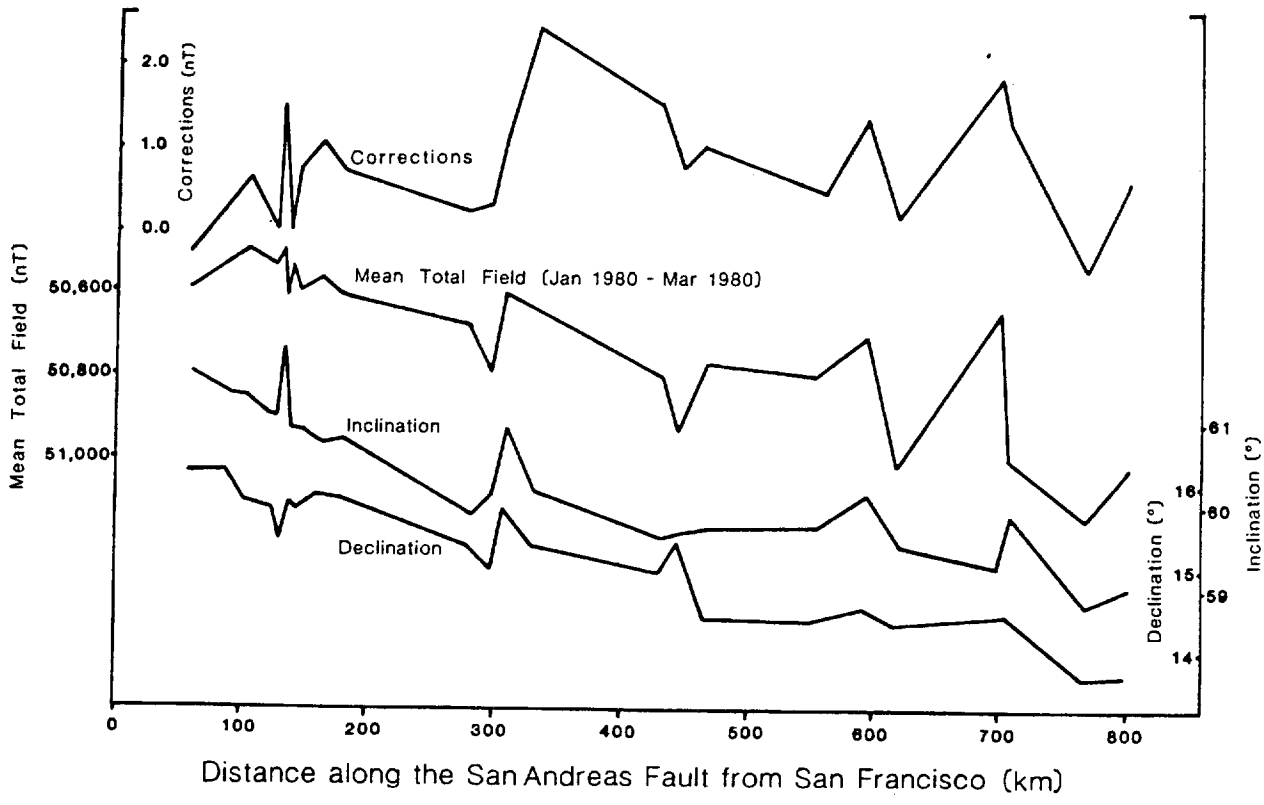

Fig. 3. Plot of site correction values, inclination, declination, and mean geomagnetic field (January to March 1980) as a function of distance along the San Andreas fault from San Francisco.

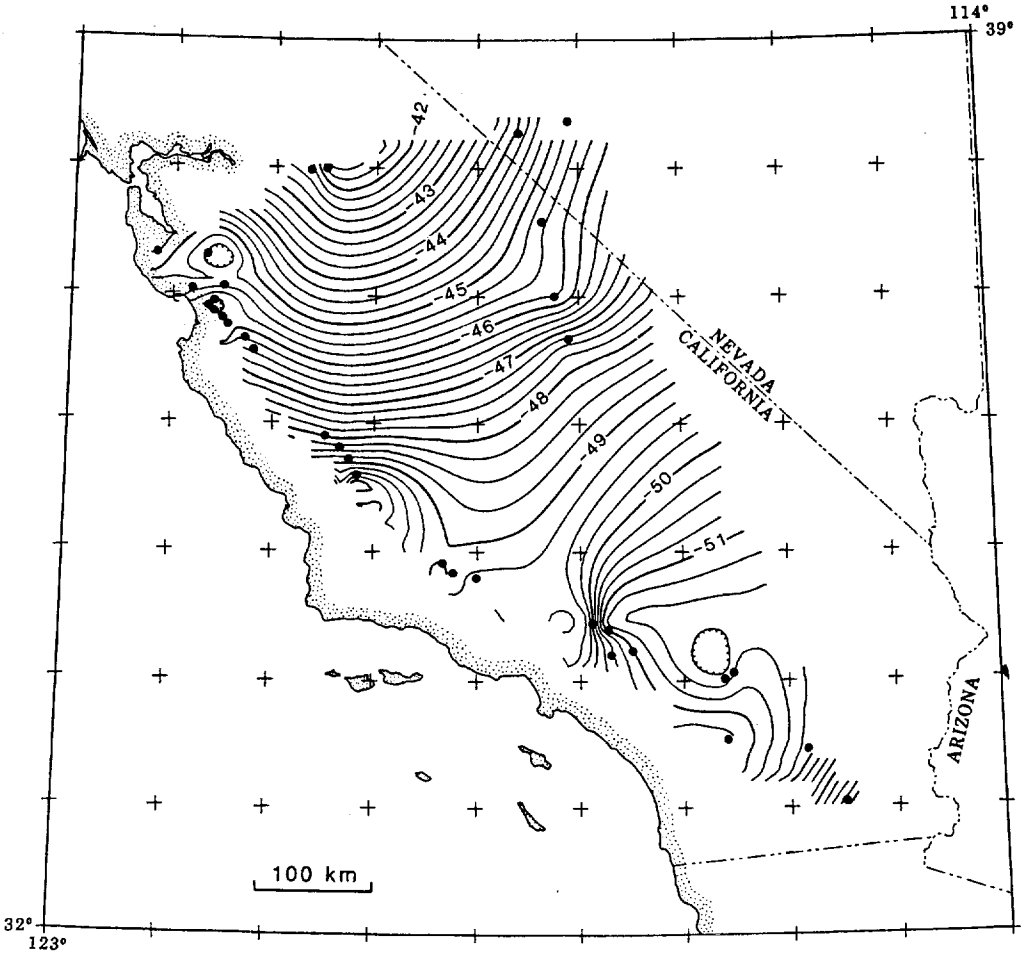

Fig. 4*a*. Minimum total curvature contour fit to observed total field secular variation data obtained along the San Andreas fault with a contour interval of 0.25 nT/a. A grid interval of 30 km was chosen to minimize high-order fitting in regions of high station density.

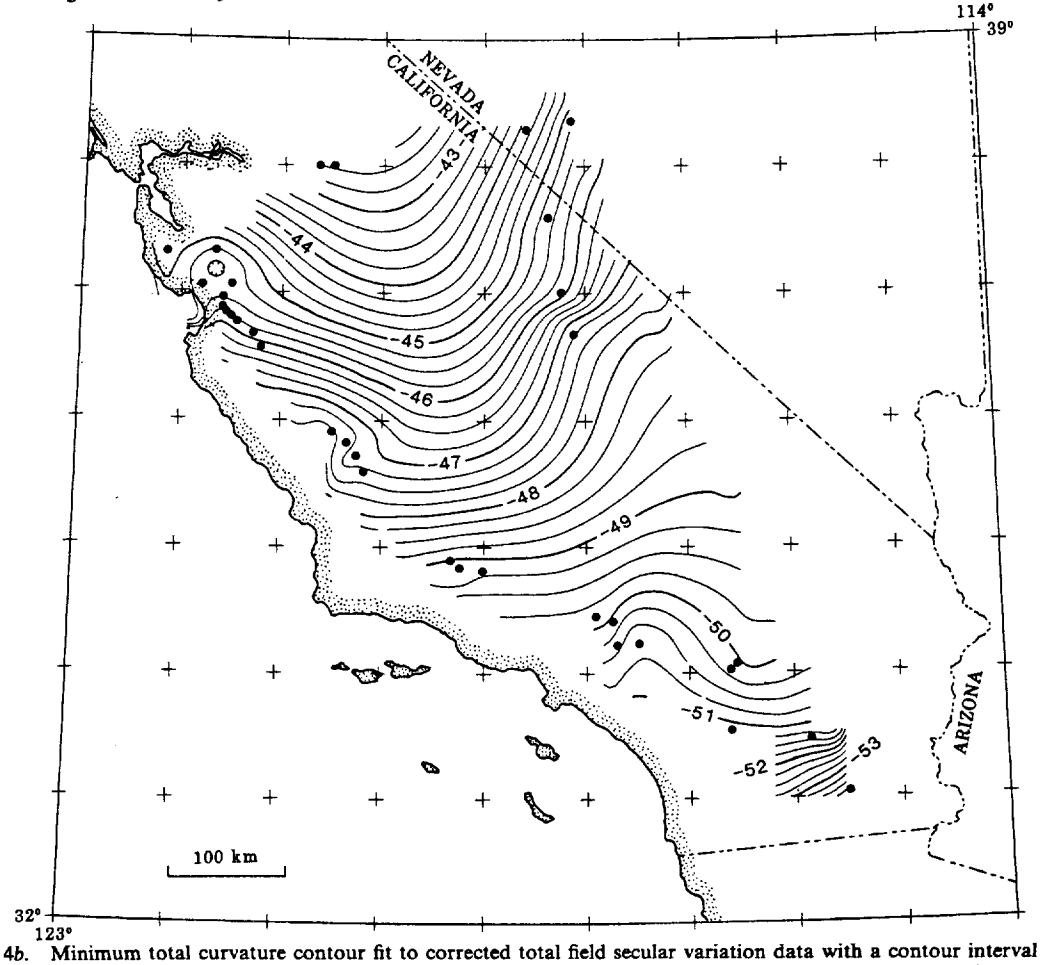

Fig. 4*b*. Minimum total curvature contour fit to corrected total field secular variation data with a contour interval 0.25 nT/a. A grid interval of 30 km was chosen to minimize high-order fitting in regions of high station density.

TABLE 2. Geomagnetic Field Coefficients, Corrected Component Data Relative to Site HAR, and Inclination and Declination Measurements for Sites in California

Site	A	$\dot{X}$, nT/a	B	$\dot{Y}$, nT/a	C	$\dot{Z}$, nT/a	Declination, deg	Inclination, deg
BLM	0.4373	−25.48	0.0144	−26.84	1.0815	−30.94	16.198	61.637
MTH	0.4421	−25.77	0.0000	−27.14	1.1227	−30.29	16.206	61.381
COY	0.4459	−26.11	−0.0186	−27.51	1.0910	−31.71	15.979	61.339
EUC	0.4554	−26.11	−0.0308	−27.51	1.0767	−31.71	15.833	61.393
SAR	0.4657	−26.17	−0.0533	−27.56	1.0934	−31.77	16.150	61.143
ANZ	0.4365	−26.23	−0.0097	−27.63	1.0619	−31.85	15.415	61.904
SNJ	0.4433	−26.27	−0.0020	−27.67	1.0771	−31.90	15.771	61.157
SJN	0.4418	−26.34	−0.0085	−27.74	1.0525	−31.98	15.825	61.984
HAR*	0.4276	−26.43	0.0151	−27.84	1.0662	−32.09	15.727	60.951
LEW	0.4406	−26.61	−0.0029	−28.03	1.0551	−32.32	15.909	60.797
BVL	0.4362	−26.75	−0.0050	−28.17	1.0658	−32.48	15.878	60.847
LGC	0.4414	−27.78	−0.0449	−29.26	1.0869	−33.73	15.303	59.932
GDH	0.4337	−27.95	−0.0379	−29.44	1.0738	−33.94	15.042	60.197
AGD	0.4434	−28.09	−0.0307	−29.59	1.0548	−34.11	15.771	60.946
GRA	0.4376	−28.23	−0.0399	−29.73	1.0510	−34.27	15.304	60.200
STG	0.4579	−29.39	−0.0506	−30.96	1.0346	−35.68	14.983	59.670
ABL	0.4366	−29.49	−0.0584	−31.07	1.0648	−35.81	15.366	59.704
CHU	0.4174	−29.68	−0.0686	−31.26	1.0827	−36.04	14.424	59.764
PAL	0.3993	−30.71	−0.0639	−32.35	1.0599	−37.29	14.403	59.736
BUR	0.3915	−30.87	−0.0671	−32.52	1.0695	−37.48	14.568	60.171
LRS	0.4009	−31.19	−0.0708	−32.85	1.0714	−37.87	14.391	59.571
SSK	0.4279	−31.21	−0.0719	−32.88	1.0391	−37.90		
LSB	0.3573	−32.04	−0.0527	−33.75	1.0366	−38.91	14.482	59.893
OCH	0.3753	−32.03	−0.0562	−33.74	1.0233	−38.89	14.437	59.336
TAB	0.3762	−32.38	−0.0535	−34.10	1.0379	−39.31	13.731	58.869
BCB	0.3884	−33.04	−0.0897	−34.80	1.0369	−40.11	13.728	59.074

*Reference site.

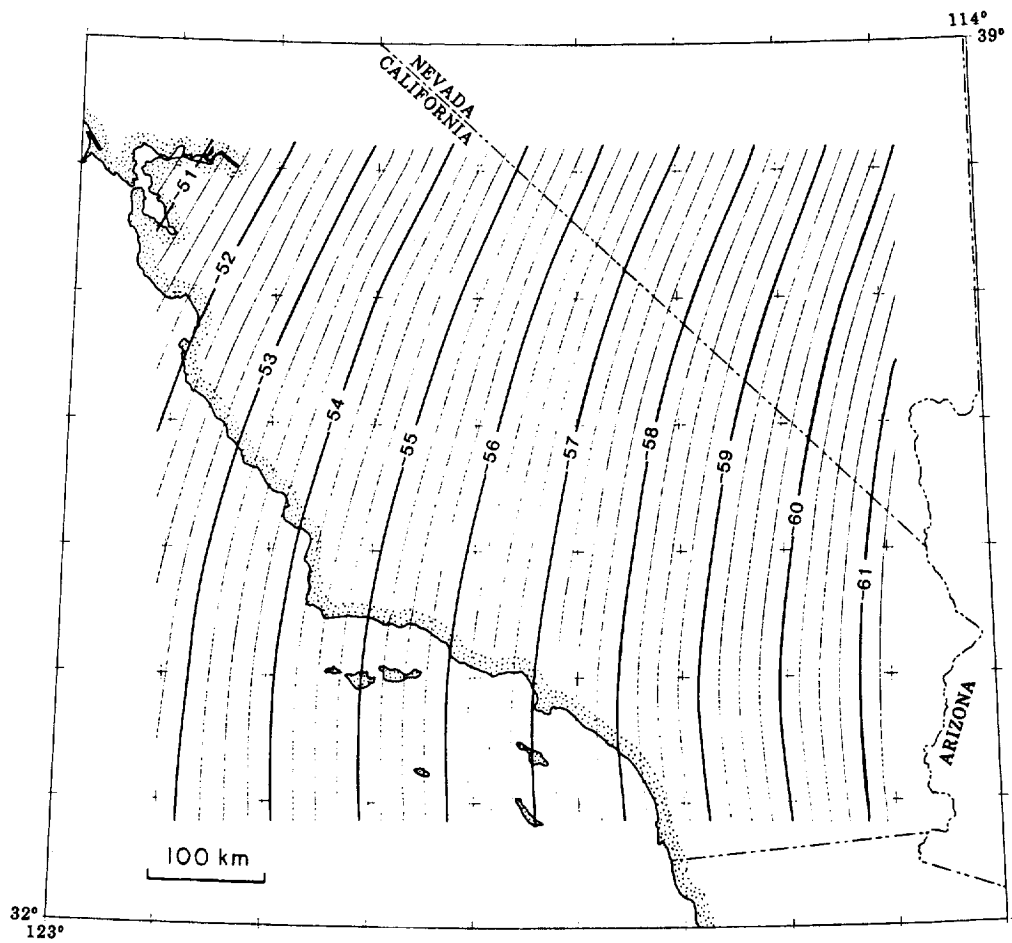

Fig. 5a. Total field secular variation calculations for central and southern California obtained with a contour interval of 0.25 nT/a from the PGRF79 model [*Peddie*, 1982].

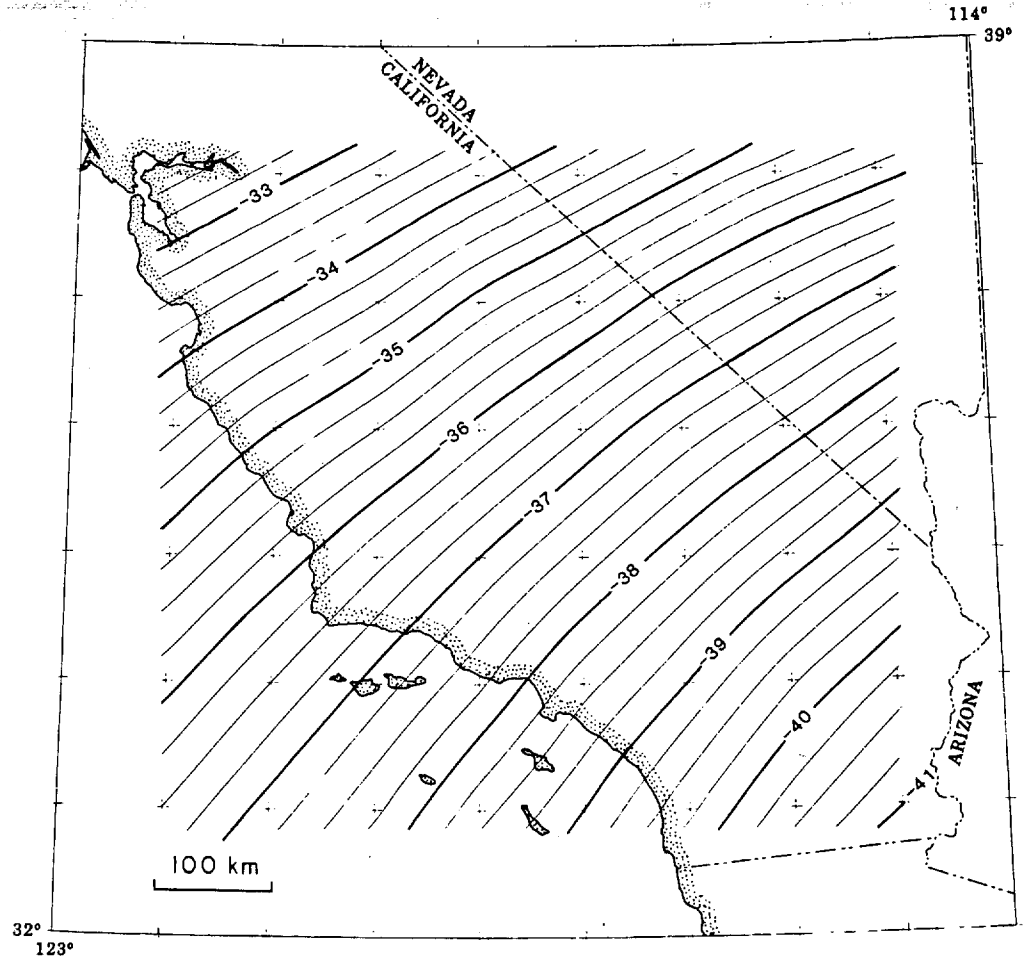

Fig. 5b. Total field secular variation calculations for central and southern California obtained with a contour interval of 0.25 nT/a from the MAGSAT model MO51782 [*Cain et al.*, 1984].

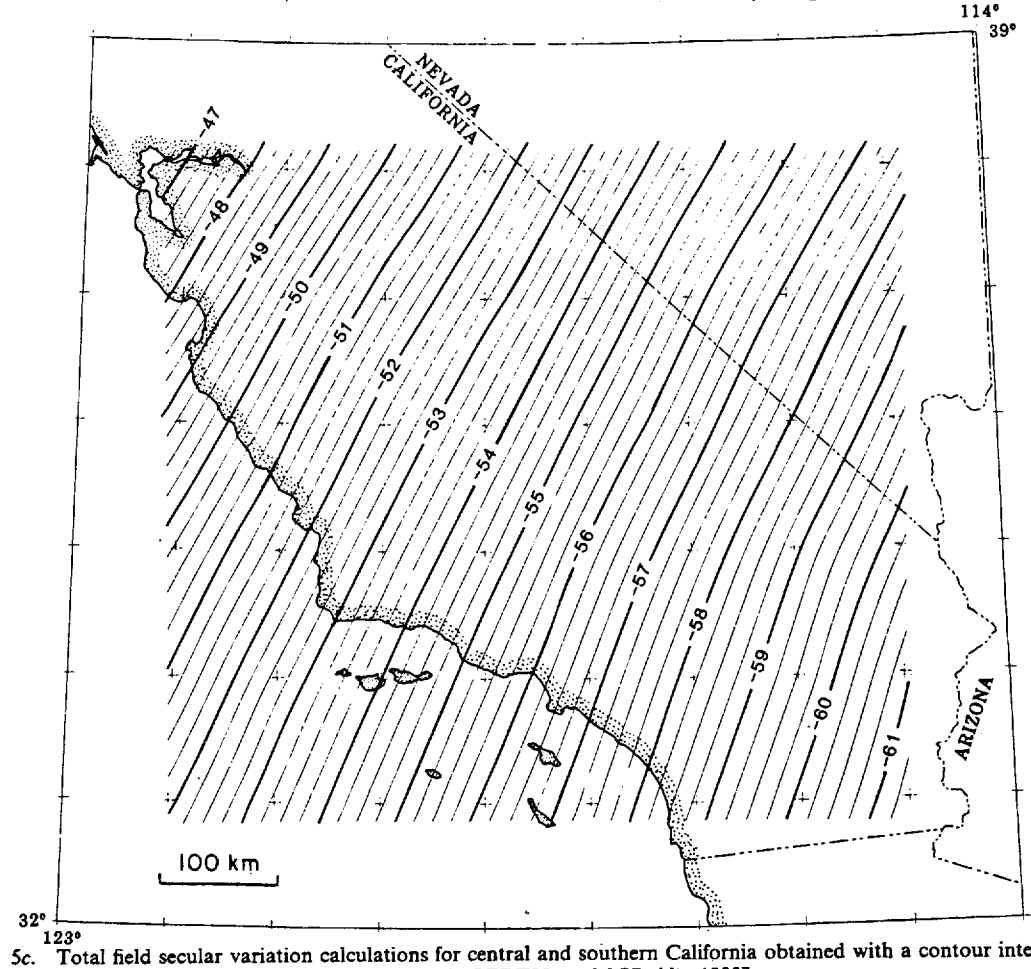

Fig. 5c. Total field secular variation calculations for central and southern California obtained with a contour interval of 0.25 nT/a from the IGRF80 model [*Peddie*, 1982].

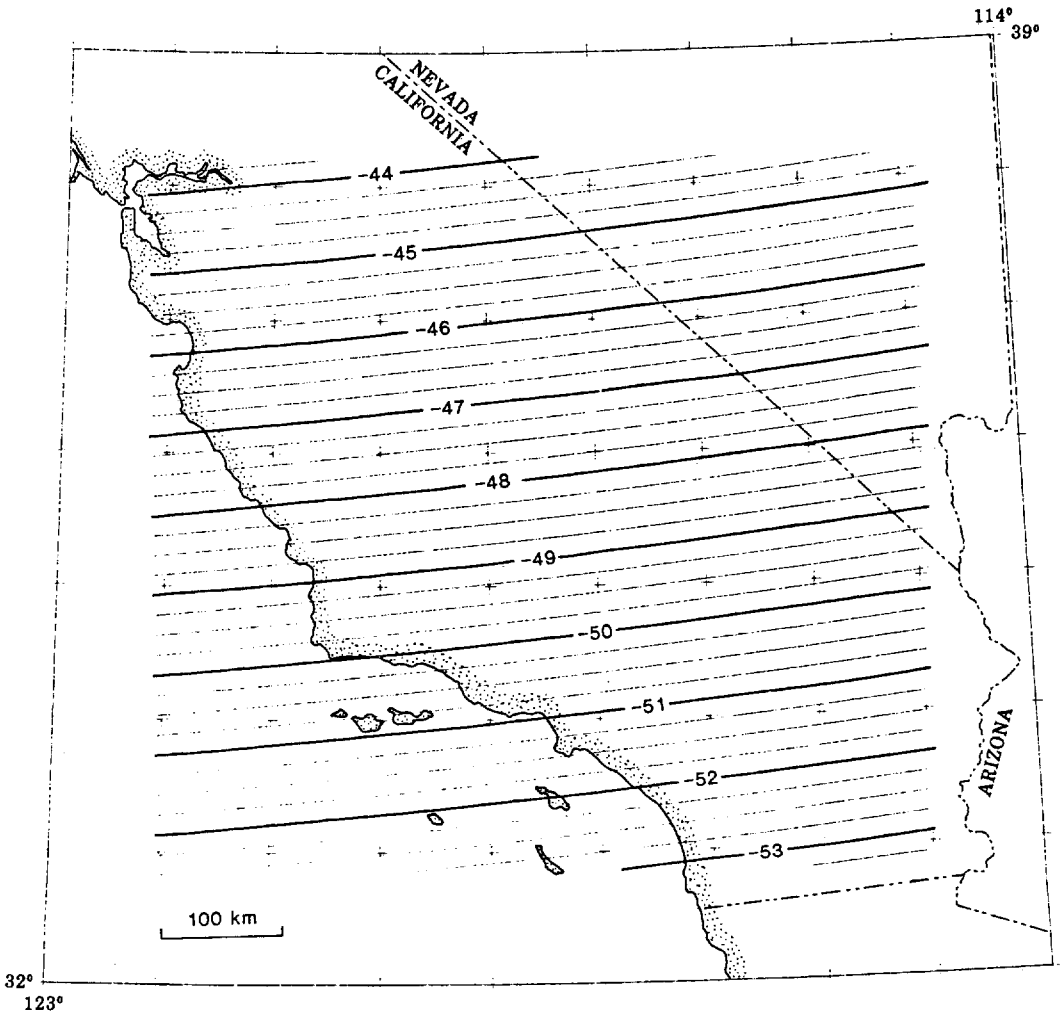

Fig. 6a. Least squares planar fit to uncorrected total field data from the California array with a contour interval of 0.25 nT/a.

detrended field components from HAR, and A, B, and C are the zero-lag Wiener filter coefficients. If the field changes uniformly over a period of time, it follows that $\dot{F}_i \approx A\dot{X}_i + B\dot{Y}_i + C\dot{Z}_i$. Before calculation of the coefficients the component data and their first derivatives were corrected for latitude variation of storm amplitudes obtained by a least squares analysis of storm amplitudes across the whole array. The values of the coefficients and the $\dot{X}$, $\dot{Y}$, and $\dot{Z}$ values obtained are listed for the different sites in Table 2 together with the values of inclination and declination at each site. We note a general correspondence (see Figure 3) between local correction terms that differ significantly from zero, anomalous inclination values, declination values, and the magnetization state of the rocks, as indicated by mean total field at each site, or more crudely, by magnetic anomaly maps of the area. Generally, in regions of significant crustal magnetization (e.g., ANZ, AGD, BUR, etc.), there is significant distortion of the geomagnetic field, and a correction must be made for these effects.

5. Corrected Secular Variation Data

An improved set of secular variation values were obtained using the coefficients in Table 2 and the corrected HAR three-component data. These values are included in Table 1 together with the errors in each determination, the amount of correction required at each site, and the residual values obtained, as we will see later, by subtracting a planar fit to the corrected data. The corrected data were fit with the contour plotting routine in the same way as described for Figure 4a. The grid interval was again chosen to be 30 km. The results are plotted in Figure 4b. An important feature of Figure 4b is the reduction of apparent small-scale secular variation along the San Andreas fault where the permanent telemetered stations give the highest site density and the best data quality. Sites for which no corrections could be made (e.g., sites N1M and N2M in the northeast) still show apparent small-scale secular variation anomalies.

6. Secular Variation Models

Various geomagnetic reference field models have been developed from spherical harmonic analyses of global observatory data. The models allow prediction of and correction for secular variation in various epochs at arbitrary points on the earth's surface [*Peddie*, 1981, 1982; *Cain et al.*, 1983, 1984]. The detailed secular variation measurements from the California array can be used in conjunction with model predictions to estimate the accuracy of the various models in this region.

The various models PGRF79, IGRF80, Magsat, etc. do refer to different time periods within the total period we are considering here. However, the observed data (Figure 2) show that the character of secular variation has not changed during this total time period, so we can validly compare the predictions of the various models, both between themselves and with

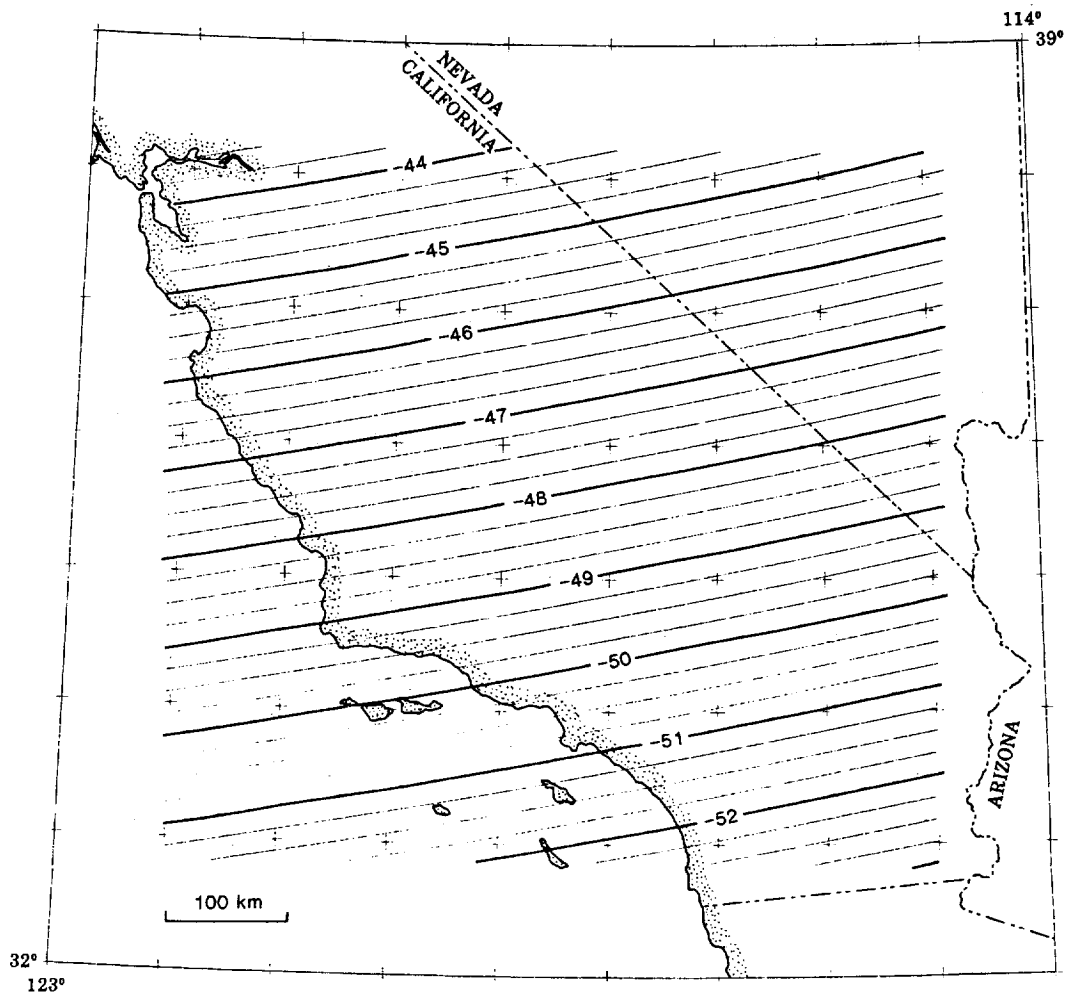

Fig. 6b. Least squares planar fit to corrected total field data from the California array with a contour interval of 0.25 nT/a.

the observed data. Calculations from the PGRF79, Magsat (MO51782), and IGRF80 models for the region spanned by the California array are shown in Figures 5a, 5b, and 5c. The models obviously do not agree with each other, and, if we compare these plots with the uncorrected and corrected observations in Figures 4a and 4b, they do not agree with the observed data either. While prediction of the detailed "small-scale" variation would not be expected from global models, the general amplitude and sense would be expected to be in agreement with the observations.

In order to make a better general comparison between the observed data and the various model predictions, the detail on Figures 4a and 4b was suppressed by computing a first-order least squares planar fit to the data. The planar surface which best fits the uncorrected array data is shown in Figure 6a. This surface describing the rate of change of total field with time, $\dot{F}$, can be expressed by an equation of the form

$$\dot{F} = k_1 * \theta + k_2 * \phi + K \qquad (2)$$

where θ and ϕ are the geographic latitude and west longitude (negative), respectively, k_1 is 1.66 ± 0.13 nT/a deg, k_2 is -0.13 ± 0.10 nT/a deg, and K is -123.2 ± 0.2 nT/a, respectively, and the coefficient of determination is 0.9997. Almost the same equation is obtained if the southern California data are omitted in order to test the solution robustness with a more uniformly distributed data subset.

The planar surface which best fits the corrected array data is shown in Figure 6b. Its equation has the form

$$\dot{F} = k_1 * \theta + k_2 * \phi + K \qquad (3)$$

where k_1, k_2, and K are now 1.50 ± 0.08 nT/a deg, -0.23 ± 0.06 nT/a deg, and -129.2 ± 0.12 nT/a, respectively.

Comparison of the predicted and observed secular variation indicates that discrepancies of several tens of nanoteslas per year and several tens of degrees occur. It seems unlikely that the present models could be used successfully to correct for secular variation in this region.

The residual field variations after removal of the general secular variation can be obtained by subtracting values calculated from equation (3) from the corrected rates at each site. The residual values obtained in this way are listed in Table 1. Figure 7 shows a contour fit to these residuals calculated with the same parameters as for Figure 4a. Note that because of the paucity of stations and because N1M and N2M are on the Sierra Nevada frontal range magnetic anomaly [*Blake et al.*, 1977], the apparent anomaly in the Great Valley is poorly determined and not significant. If complete site corrections have been successfully accomplished, then these residuals are generated by physical processes other than those related to external magnetospheric and ionospheric disturbances or sources in the core. Since each of the regions of greatest residuals on the San Andreas fault is a region of anomalous

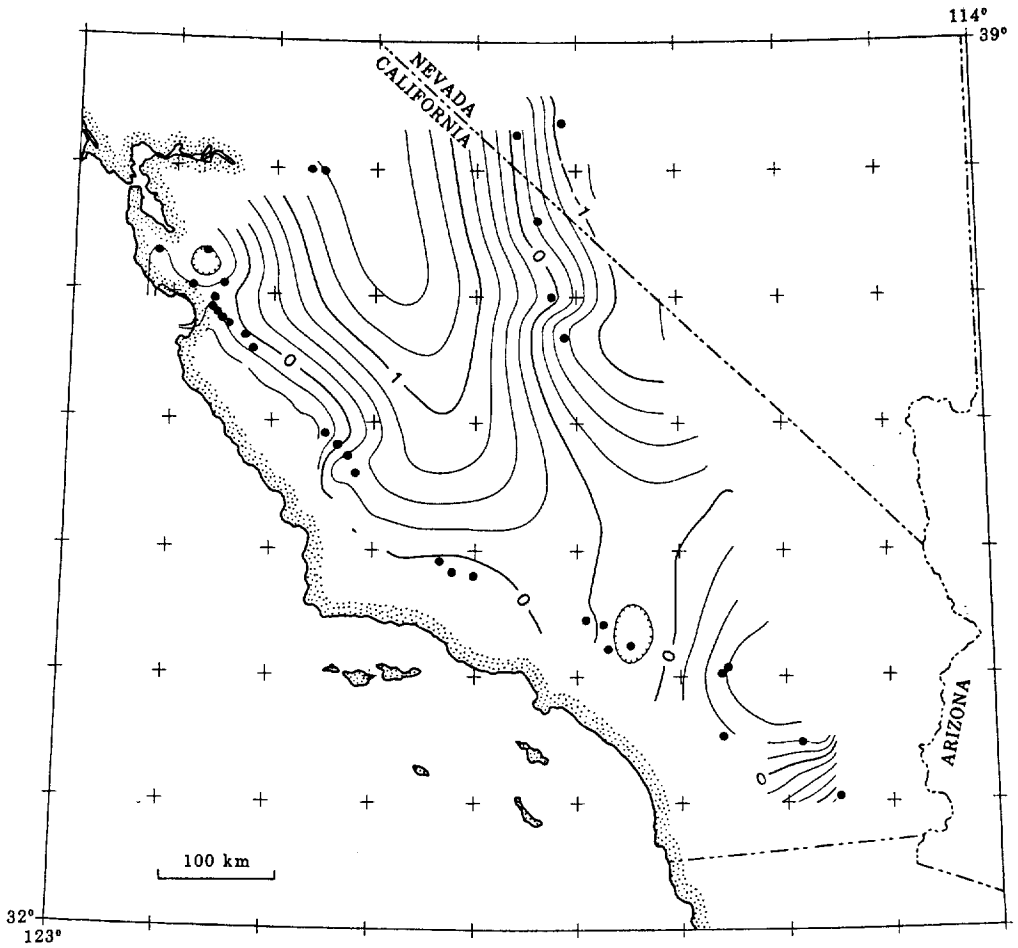

Fig. 7. Residual total field secular magnetic field changes not apparently related to sources in the core or the magnetosphere obtained by subtraction of Figure 6*b* from Figure 4*b*. The contour interval and the grid spacing are again 0.25 nT/a and 30 km, respectively. Note that because of the paucity of stations and because N1M and N2M are on the Sierra Nevada frontal range magnetic anomaly [*Blake et al.*, 1977], the apparent anomaly in the Great Valley is poorly determined and not significant.

tectonic and seismic behavior, some contribution from tectonomagnetic sources might be expected.

7. Discussion

Five to ten years of total field proton precession data from 34 sites across California are used to define the characteristics of secular variation between latitudes 33° to 38°N and longitudes 115° and 122°W. The observed secular variation decreases uniformly with time during this period. The values at each site are well determined and range from −45 nT/a near San Francisco to −54 nT/a near the Mexican border with the error in determination of these rates typically less than 0.2 nT/a.

These data show general agreement from site to site in the linear form of the secular variation, but sites only a few kilometers apart can have rates which differ by as much as 1.0 nT/a. This is most easily demonstrated by the resulting scatter about a least squares planar fit to the data or by the need to use high-order surfaces to fit all of the data. The regions near San Juan Bautista (SJN in Figure 1) and Parkfield (GDH in Figure 1) are densely instrumented because they are the most tectonically active and geologically complex. Data from these regions show the most scatter about the mean value of secular variation in each place.

Since the magnetic field at a particular site resulting from the application of a uniform or nonuniform external field perturbation is a function of the local induced and remanent magnetization vectors at that site, the same applied field will produce a different net field vector at different sites. While these site response effects are not a serious problem in general magnetic surveying experiments, they are of concern in this study. Correction for these effects is necessary before valid comparisons of precise field values can be made between sites. A preliminary determination of site response effects in the California data was made by calculating the Wiener filter coefficients which best mapped three-component data during magnetic storms at one site into the total field data at each of the other sites in the manner described by *Davis and Johnston* [1983]. Corrected secular variation values were obtained using these coefficients at each site with continuous field data. The results, while not ideal, represent the best estimates of secular variation in this region yet obtained.

The corrected data were fit with a planar surface. Some scatter about this surface is still apparent, and a question still exists whether the site response corrections could be further improved, or whether the residual changes are secular changes of tectonic origin. HAR, the only site with a three-component magnetometer, is on a granite batholith with quite low magnetic remanence and susceptibility [*Hanna et al.*, 1972] but is near the San Andreas fault where the geology is complex. Current channeling apparently occurs along the fault zone [*Johnston et al.*, 1983]. Better results might be obtained by

using data from the automatic three-component magnetometer run by the USGS at Fresno, California [*Alldredge*, 1983], and from other three-component systems scattered through the array.

On the other hand, the largest residual near the San Andreas fault, shown in Figure 7 after the data are corrected for secular variation, occurs in the region of the San Andreas fault system southeast of Palm Springs near OCH to the Salton Sea near BCB (Figure 1). Smaller, less significant residuals occur on the southern Hayward/Calaveras fault system (MTH) and just to the south of Parkfield (GDH). In these locations, temporal change in crustal stress and stress localization is expected. In fact, two of the largest four earthquakes in California during the last 10 years have occurred within the northern anomaly. These earthquakes are the Coyote earthquake of August 6, 1979 ($M_L = 5.9$), and the Morgan Hill earthquake of April 24, 1984 ($M_L = 5.8$), which occurred near sites COY and MTH, respectively (Figure 1). No moderately large earthquakes have yet occurred within the southern anomaly. The amplitude of the residual (≈ 0.75 nT/a) is comparable to signals expected from tectonomagnetic models of these areas [*Johnston*, 1978]. If the models are correct, a damaging earthquake might therefore be expected in the region of the southern anomaly in the near future. However, without independent data to support this possibility, it cannot be pursued further at this point. An alternative but less likely explanation is that correction for site effects is not yet complete. Data from a few three-component magnetometers through the array would clarify this.

Neither the corrected nor the uncorrected data agree well with the current secular variation models. While the models were not designed for precise predictions on such a small scale, agreement was expected with the general form and amplitude of secular variation measured with the array. This is clearly not the case. While better results may be obtained in other regions, the differences between observations and predictions obtained here are so large that they preclude use of any of the present models for independent prediction and removal of secular variation from the array data. More importantly, if these data were from various observatories around the world, the use of spherical harmonic expansions to fit the data would clearly produce distorted results.

It is possible that some of the observatory data used to construct the global models are contaminated by effects of local induction and remanent magnetization and that these are biasing the models. If so, similar analyses could be applied to each of the magnetic observatories to determine which are in regions where distortion of the measured geomagnetic field values might be expected. Significant improvements in the coefficients of spherical harmonic fits to global data could result, and this might explain some of the discrepancies between observations and models reported here.

Acknowledgments. J. C. Cain kindly ran the secular variation models and provided the data for Figures 5*a*, 5*b*, and 5*c*. The manuscript benefited from useful comments by R. W. Simpson and L. R. Alldredge.

REFERENCES

Alldredge, L. R., Main field and recent secular variation, *Rev. Geophys.*, *21*, 599–603, 1983.

Blake, M. C., I. Zietz, and D. L. Daniels, Aeromagnetic and generalization geologic map of parts of central California, U.S. Geol. Surv. Map, *GP-918*, 1977.

Briggs, I. C., Machine contouring using minimum curvature, *Geophysics*, *39*, 39–48, 1974.

Bullard, E. C., C. Freedman, H. Gellman, and J. Nixon, The westward drift of the earth's magnetic field, *Philos. Trans. R. Soc. London, Ser. A*, *243*, 67–79, 1950.

Cain, J. C., J. Frayser, L. Muth, and D. Schmitz, The use of Magsat data to determine secular variation, *J. Geophys. Res.*, *88*, 5903–5910, 1983.

Cain, J. C., D. R. Schmitz, and L. Muth, Small-scale features in the earth's magnetic field observed by Magsat, *J. Geophys. Res.*, *89*, 1070–1076, 1984.

Chapman, S., and J. Bartels, *Geomagnetism*, Clarendon, Oxford, 1940.

Davis, P. M., and M. J. S. Johnston, Localized geomagnetic field changes near active faults in California 1974–1980, *J. Geophys. Res.*, *88*, 9452–9460, 1983.

Davis, P. M., D. D. Jackson, C. A. Searls, and R. L. McPherron, Detection of tectonomagnetic events using multichannel predictive filtering, *J. Geophys. Res.*, *86*, 1731–1737, 1981.

Elasser, W. M., The earth's interior and geomagnetism, *Rev. Mod. Phys.*, *22*, 876–893, 1950.

Hanna, W. F., R. D. Brown, D. C. Ross, and A. Griscom, Aeromagnetic reconnaissance and generalized geologic map of the San Andreas fault between San Francisco and San Bernardino, California, *U.S. Geol. Surv. Geophys. Invest. Map*, *GP-815*, 1972.

Johnston, M. J. S., Local magnetic field variations and stress changes near a slip discontinuity, *J. Geomagn. Geoelectr.*, *30*, 511–522, 1978.

Johnston, M. J. S., B. E. Smith, and R. Mueller, Tectonomagnetic experiments and observations in western U. S. A., *J. Geomagn. Geoelectr.*, *28*, 85–97, 1976.

Johnston, M. J. S., R. H. Ware, and R. Mueller, Tidal-current channeling in the San Andreas fault, California, *Geophys. Res. Lett.*, *10*, 51–54, 1983.

Johnston, M. J. S., R. J. Mueller, R. H. Ware, and P. M. Davis, Precision of geomagnetic field measurements in a tectonically active region, *J. Geomagn. Geoelectr.*, *36*, 83–95, 1984.

Langel, R., J. Berbert, T. Jennings, and R. Horner, Magsat data processing: A report for investigators, *NASA Tech. Memo.*, *TM-82160*, Nov. 1981.

Mueller, R. J., M. J. S. Johnston, B. E. Smith, and V. Keller, U.S. Geological Survey magnetometer network and measurement techniques in western U. S. A., *U.S. Geol. Surv. Open File Rep.*, *81-1346*, 1981.

Peddie, N. W., International Geomagnetic Reference Field 1980: A report by IAGA division 1, working group 1, *J. Geomagn. Geoelectr.*, *33*, 607–611, 1981.

Peddie, N. W., International Geomagnetic Reference Field: The third generation, *J. Geomagn. Geoelectr.*, *68*, 265–268, 1982.

Peddie, N. W., and E. B. Fabiano, A proposed international geomagnetic reference field for 1965–1985, *J. Geomagn. Geoelectr.*, *34*, 357–364, 1982.

Prescott, W. H., J. C. Savage, and W. T. Kinoshita, Strain accumulation rates in the western United States between 1970 and 1978, *J. Geophys. Res.*, *84*, 5423–5436, 1979.

Regan, R. D., J. C. Cain, and W. M. Davis, A global magnetic anomaly map, *J. Geophys. Res.*, *80*, 794–802, 1975.

Shapiro, V. A., and M. J. S. Johnston, Symposium on Tectonomagnetics and Small Scale Secular Variation, Seattle, August 22, 1977, *Adv. Earth Planet. Sci.*, *5*, 1–2, 1979.

Stacey, F. D., and M. J. S. Johnston, Theory of the piezomagnetic effect in titanomagnetite-bearing rocks, *Pure Appl Geophys.*, *97*, 146–155, 1972.

Yukutake, T., and H. Tachinaka, Separation of the earth's magnetic field into drifting and standing parts, *Bull. Earthquake Res. Inst. Univ. Tokyo*, *47*, 65–97, 1969.

K. S. Breckenridge, M. J. S. Johnston, R. J. Mueller, and S. A. Silverman, U.S. Geological Survey, Menlo Park, CA 94025.

(Received September 11, 1984;
revised April 16, 1985;
accepted April 18, 1985.)